Direct Measurements of the Mechanical Stability of Zinc-Thiolate Bonds in Rubredoxin by Single-Molecule Atomic Force Microscopy

Peng Zheng and Hongbin Li*
Department of Chemistry, University of British Columbia, Vancouver, British Columbia, Canada

ABSTRACT Zinc (Zn) is one of the most abundant metals and is essential for life. Through ligand interactions, often with thiolate from cysteine residues in proteins, Zn can play important structural roles in organizing protein structure and augmenting protein folding and stability. However, it is difficult to separate the contributions of Zn-ligand interactions from those originating from intrinsic protein folding in experimental studies of Zn-containing metalloproteins, which makes the study of Zn-ligand interactions in proteins challenging. Here, we used single-molecule force spectroscopy to directly measure the mechanical rupture force of the Zn-thiolate bond in Zn-rubredoxin. Our results show that considerable force is needed to rupture Zn-thiolate bonds (~170 pN, which is significantly higher than the force necessary to rupture the coordination bond between Zn and histidines). To our knowledge, our study not only provides new information about Zn-thiolate bonds in rubredoxin, it also opens a new avenue for studying metal-ligand bonds in proteins using single-molecule force spectroscopy.

INTRODUCTION

Zinc (Zn) is one of the most abundant, pervasive, and important metals in life. There are ~2800 Zn(II)-binding human proteins, constituting ~10% of the proteome (1–5). Zn is a nonredox metal that plays important structural roles in metalloproteins. By interacting with its ligands, the Zn site plays an important structural role in proteins, organizing tertiary and quaternary structures, and augmenting protein folding and stability (5,6). Thus, understanding the interactions between Zn and its protein ligands (mainly the side chains of amino acid residues) is imperative for elucidating the structural role of Zn in proteins and how nature uses different metals to accomplish different functions.

Studies using traditional coordination chemistry methods to examine metalloproteins and simple synthetic analogs (structural mimics) have provided tremendous insights into Zn-ligand interactions at the ensemble level, including the metal-binding free energy, affinity, selectivity, and the bond dissociation/association rate (6–11). However, in studies of metalloproteins, the energetic contributions from Zn-ligand interactions are inevitably mixed with those from the protein itself, which makes it difficult to elucidate the physical properties of Zn-ligand interactions in proteins (8). However, over the last two decades, the development of single-molecule force spectroscopy techniques has provided a promising new avenue for investigating such metal-ligand interactions.

The atomic force microscopy (AFM)-based force spectroscopy technique is a simple but powerful experimental tool for investigating the mechanical and kinetic properties of chemical bonds along a reaction coordinate predefined by the applied force (12–14). By applying a stretching force to the chemical bond of interest, one can accelerate the bond dissociate rate exponentially (15,16), leading to the mechanical rupture of the chemical bond. By measuring the mechanical rupture force of chemical bonds, one can determine their mechanical stability and unbinding kinetics. Over the last two decades, many different types of chemical bonds and interactions, including covalent bonds and coordination bonds, have been studied by AFM (13,17,18). These efforts have paved the way for the rapid development of mechanochemistry (13,19,20). Investigators have mainly examined interactions between Zn and its ligands using a nitrilotriacetic acid (NTA)-His-tag system (21–23); however, Zn-ligand interactions in Zn-containing metalloproteins remain largely unexplored.

In a recent study, we combined single-molecule AFM and protein engineering techniques to investigate ferric (Fe)-thiolate bonds in a simple metalloprotein, rubredoxin (RD) (24). We discovered that the highly covalent Fe-thiolate bond is mechanically labile and ruptures at forces well below those of typical covalent bonds. In this study, we demonstrated the feasibility of studying metal-ligand bonds in proteins. Moreover, because RD can accommodate a wide variety of metal ions (25), this study also established a valuable platform for investigating different metal-thiolate bonds in proteins. Here, we used this methodology to investigate Zn-thiolate bonds in RD as part of our efforts to understand the mechanical stability of metal-ligand coordination bonds in metalloproteins, particularly for biologically relevant metals such as Zn.

We chose Zn-substituted RD from Pyrococcus *furiosus* (Zn-*pf*RD) as a model system for studying the mechanical stability of Zn-thiolate bonds in metalloproteins. The wild-type RD is a soluble Fe-S protein with low molecular mass (~6 kDa). It contains one Fe ion coordinated with four cysteine residues arranged within two CXXC chelating

Submitted June 10, 2011, and accepted for publication August 9, 2011.

*Correspondence: Hongbin@chem.ubc.ca

Editor: Peter Hinterdorfer.

© 2011 by the Biophysical Society

0006-3495/11/09/1467/7 $2.00

doi: 10.1016/j.bpj.2011.08.021

motifs (26). When RD is overexpressed in *Escherichia coli*, a considerable amount of Zn-substituted RD is naturally produced (27). The structure of Zn-*pf*RD, revealed by NMR and x-ray diffraction techniques, shows a metal-binding site (Fig. 1 *A*) identical to that in Fe-*pf*RD (28,29). Of interest, the coordination geometry of the ZnS_4 site in Zn-RD is highly similar to that of naturally occurring Zn-containing proteins, despite differences in their global folds. For example, alcohol dehydrogenase, DNA polymerase II, and the Ada DNA repair protein all have this ZnS_4 center with similar tetrahedral geometry, in which the four cysteines residues are arranged into two CX_nC motifs ($n = 2$–4) (4,7,8,30,31). Fig. 1 *B* shows the global structure and the ZnS_4 site of the Ada DNA repair protein. It is clear that Zn-*pf*RD and the Ada DNA repair protein show high similarities in their ZnS_4 centers (31). It is noted that the ZnS_4 is the most common Zn center in Zn-containing proteins (amounting to ~40%), and acts mainly as a structural site (3). Furthermore, cysteine is the most common ligand for Zn, with nearly all Zn centers in proteins containing a cysteine ligand (>90%) (1,3,32). Thus, we chose the ZnS_4 site in Zn-*pf*RD as a model system to study its mechanical stability, as well as to demonstrate the potential of using the single-molecule AFM technique to study metal-ligand interactions in metalloproteins.

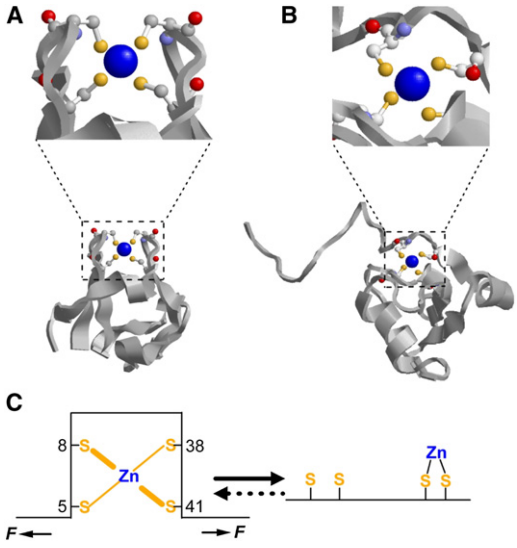

FIGURE 1 (*A*) Three-dimensional structure of Zn(II)-*pf*RD (PDB code: 1ZRP). The inset shows the Zn coordination site in which the Zn ion is coordinated by four cysteinyl sulfur atoms arranged in a pseudo-tetrahedral environment. The Zn atom and the four cysteines are highlighted in ball-and-stick representation. (*B*) The NMR structure of Ada DNA repair protein (PDB code: 1ADN). Although the Ada DNA repairing protein and Zn-*pf*RD have different three-dimensional structures, both proteins show highly similar ZnS_4 centers. (*C*) Schematics of the mechanical rupture of Zn-thiolate bonds in Zn-*pf*RD. The stretching force is applied to Zn-*pf*RD through the N- and C-termini of the protein. When Zn-thiolate bonds (at least two from the same CXXC chelating motif) rupture, residues 5–41 are exposed to the stretching force. The dashed line indicates the possibility of refolding of Zn-*pf*RD and reconstituting the Zn-S_4 center.

MATERIALS AND METHODS

Protein engineering

A plasmid containing the gene of *pf*RD was kindly provided by Dr. Eidsness. The gene encoding the protein chimera cys-*pf*RD-GB1-cys was constructed in pQE80L (Qiagen, Valencia CA) and transformed into the *Escherichia coli* strain DH5α by means of standard molecular biology techniques (GB1 is the B1 IgG-binding domain of protein G from *Streptococcus*, and is used as a fingerprint for identifying single-molecule stretching events in AFM experiments). The cells were grown in M9 minimum media supplemented with 0.4% glucose, 0.1 mM $CaCl_2$, 2 mM $MgSO_4$, and 100 μg/mL ampicillin. Cultures were grown at 37°C to an OD_{600} of ~0.8, and were induced with 1 mM isopropyl β-D-1-thiogalactopyranoside (IPTG; Invitrogen, Carlsbad, CA) followed by 25 mg/mL $ZnSO_4$ (33). The protein was purified by Co^{2+}-affinity chromatography with the use of a TALON His-Tag purification resin (Clontech, Mountain View, CA). It has been shown that when RD is overexpressed in an M9 medium supplemented with Zn^{2+}, Zn-RD is the predominant form of the total expressed RD (33). Thus, a chromatographic separation step of Zn-RD from Fe-RD can be avoided. The resultant protein solution is colorless, and the UV-Vis spectrum does not show noticeable absorbance at 494 nm, confirming that Zn-RD is the dominant form of RD.

UV-Vis spectroscopy was used to quantitatively determine the purity of the Zn-*pf*RD (NanoDrop ND-1000 UV-Vis spectrometer; Thermo Scientific, Wilmington, DE). The overall protein concentration can be estimated from the sum of the extinction coefficient of GB1 (8.2 mM^{-1} cm^{-1}) and RD (25.6 mM^{-1} cm^{-1} for both the Zn and Fe forms) at 280 nm, and the concentration of Fe-form RD can be calculated from its characteristic absorbance at 494 nm (extinction coefficient = 9.2 mM^{-1} cm^{-1}). Our measurements show that the purity of Zn-form RD is >90%.

The protein solution was buffer-exchanged and concentrated to ~8 mg/mL in Tris buffer (Tris-(hydroxymethylaminomethane) at pH 7.4 using a 9K MWCO pierce concentrator (Thermo Scientific). We constructed the polyprotein $(Zn\text{-}pf\text{RD-GB1})_n$ using thiol-maleimide coupling chemistry by reacting Cys-*pf*RD-GB1-Cys with $BM(PEO)_3$(1, 8-bis-maleimido-$(PEO)_3$; Molecular Biosciences, Boulder, CO) as previously reported (34).

Single-molecule AFM experiments

All single-molecule AFM experiments were performed on a custom-built AFM at room temperature. We calibrated each MLCT Si_3N_4 cantilever (Bruker, Santa Barbara, CA) in solution before each experiment, and determined the spring constant (typically ~40 pN/nm) using the equipartition theorem. All experiments were done in 100 mM Tris buffer at pH 7.4 and at a pulling speed of 400 nm/s unless otherwise indicated.

In a typical experiment, 2 μL of the polyprotein solution (2 mg/mL) were deposited onto a clean glass coverslip covered by ~50 μL buffer and allowed to equilibrate for ~15 min before the AFM experiments were initiated.

Monte Carlo simulations

The dissociation process of the Zn-thiolate bond can be modeled as a two-state dissociation process with force-dependent rate constants. We estimated the dissociation rate constant α_0 at zero force and the distance Δx_u between the bound and transition states using Monte Carlo simulations according to published procedures (35,36). Because Zn-RD contains two CXXC Zn chelation sites (C5XXC8 and C38XXC41), the mechanical rupture of the two Zn-thiolate bonds from either CXXC site will lead to the complete unfolding of Zn-RD. Thus, the two sets of force-bearing Zn-thiolate bonds in Zn-RD can be considered to be arranged in series. This special feature, which is different from typical proteins, was taken into account in the Monte Carlo simulation.

RESULTS

Mechanical stability of Zn-thiolate bonds in the ZnS_4 center

When studying the mechanical stability of proteins using single-molecule AFM, investigators frequently use polyproteins to unambiguously distinguish single-molecule unfolding events from those of nonspecific interactions (37,38). Thus, the polyprotein (Zn-*pf*RD-GB1)$_n$ was constructed to measure the mechanical stability of Zn-thiolate bonds, where the well-characterized GB1 domains serve as a fingerprint for identifying single-molecule unfolding events of Zn-*pf*RD, as well as an internal force caliber (39,40).

Stretching the polyprotein (Zn-*pf*RD-GB1)$_n$ results in force-extension curves with a characteristic sawtooth-like pattern (Fig. 2 *B*). Each individual force peak in the curve corresponds to the mechanical unfolding of an individual domain in the polyprotein, with the last peak typically corresponding to the stretching and subsequent detachment of the fully extended polyprotein chain from either the AFM tip or the glass coverslip. Fitting the worm-like chain model of polymer elasticity (Fig. 2, *dotted lines*) (41) to the unfolding force peaks revealed that unfolding events show two different populations of contour length increment (ΔLc): one that exhibits a ΔLc of ~18 nm and one with a ΔLc of ~13 nm (Fig. 3 *A*). The mechanical unfolding of GB1 has been studied in great detail and is characterized by a ΔLc of ~18 nm (39,40). Thus, the unfolding events of ΔLc of ~18 nm can be attributed to the unfolding of GB1 domains. Accordingly, unfolding events with a ΔLc of ~13 nm can be attributed to the unfolding of Zn-*pf*RD. As we showed previously (24), the unfolding of the apo-form of RD occurs at forces below our detection limit (~20 pN). Hence, the unfolding of Zn-*pf*RD can be attributed to the rupture of the ZnS_4 center in Zn-*pf*RD, and the unfolding force of Zn-*pf*RD unfolding events reflects the mechanical stability of the Zn-thiolate bonds. This corresponds to 172 ± 58 pN (average ± standard deviation, $n = 516$) at a pulling speed of 400 nm/s (Fig. 3 *B*).

The average value of ΔLc for the unfolding of Zn-*pf*RD (12.8 ± 1.0 nm; Fig. 3 *A*) is in close agreement with that expected from the breaking of the ZnS_4 center and the subsequent unfolding of Zn-*pf*RD. As shown in Fig. 1 *C*, rupture of Zn-thiolate bonds in Zn-*pf*RD will lead to the exposure of ~37 residues between Cys-5 and Cys-41, which are shielded from the stretching force by the intact ZnS_4 center. Thus, a ΔLc of 12.4 nm (37 aa × 0.36 nm/aa – 0.9 nm) is expected for the rupture of the ZnS_4 center, consistent with experimental results. Additionally, this ΔLc value for the rupture of ZnS_4 is the same as that of the rupture of FeS_4 in Fe-*pf*RD (24), as Fe-*pf*RD and

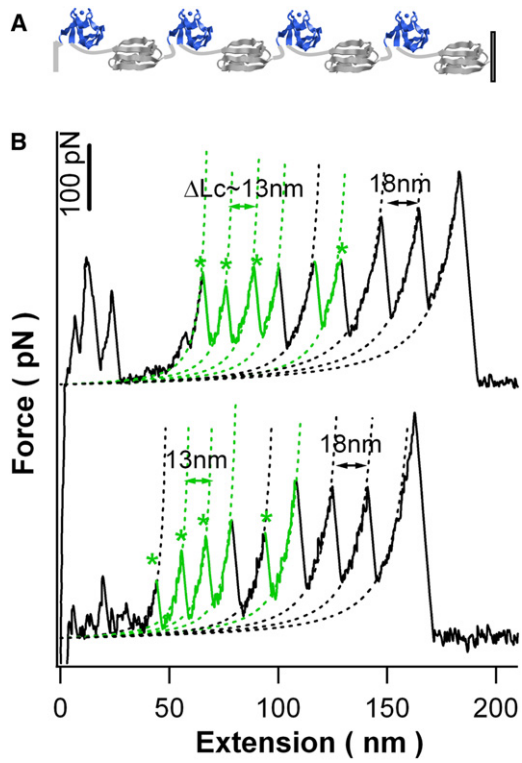

FIGURE 2 Mechanical unfolding of the polyprotein (Zn-*pf*RD-GB1)$_n$ via single-molecule AFM. (*A*) Schematics of polyprotein (Zn-*pf*RD-GB1)$_n$ stretching between cantilever and solid substrate. Zn-*pf*RD and GB1 are colored in dark and light colors, respectively. (*B*) Typical force-extension curves for the unfolding of the polyprotein (Zn-*pf*RD-GB1)$_n$ in which Zn-thiolate bonds are ruptured. The curves show characteristic sawtooth-like patterns. The unfolding force peaks can be fitted well using the worm-like chain model of polymer elasticity (*dotted lines*). Two populations of unfolding events are observed with different contour length increments. The unfolding events corresponding to a ΔLc of ~18 nm (colored in *black*) are from the mechanical unfolding of the fingerprint GB1 domains. Thus, the other unfolding events of ΔLc ~13 nm (colored in *light color* and indicated by *) can be attributed to the unfolding of Zn-RD, which is triggered by the rupture of Zn-thiolate bonds.

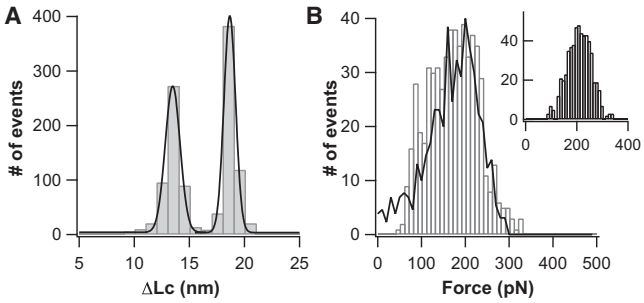

FIGURE 3 Mechanical unfolding signatures of Zn(II)-*pf*RD. (*A*) The histogram of contour length increments ΔLc of Zn(II)-*pf*RD shows a narrow distribution with an average of 12.8 ± 1.0 nm, in good agreement with the contour length increment of rupturing the Zn(II)-S_4 center and extension of the polypeptide from residues 5–41. As a reference, the ΔLc histogram for GB1 is also shown with an average of 18.2 ± 0.8 nm ($n = 576$). (*B*) Rupture-force histogram of Zn-thiolate bonds in Zn-*pf*RD shows an average of 172 ± 58 pN ($n = 516$). For comparison, the unfolding-force histogram of GB1 is shown in the inset, with an average of 208 ± 50 pN. The pulling speed was 400 nm/s. The solid line corresponds to the Monte Carlo simulation results obtained with $\alpha_0 = 0.1\ s^{-1}$ and $\Delta x_u = 0.14$ nm.

Zn-*pf*RD share a metal-binding geometry (28,29). Despite this structural similarity, it is notable that the mechanical stability of Zn(II)-thiolate bonds in *pf*RD is lower than that of Fe(III)-thiolate bonds in *pf*-RD (~210 pN), but slightly higher than that of Fe(II)-thiolate bonds (~150 pN) under similar experimental conditions (24).

The transition state for the mechanical rupture of Zn-thiolate bonds is 1.4 Å away from the bound state

As shown in Fig. 3 *B*, the rupture force of the ZnS_4 center shows a broad distribution, reflecting the stochastic nature of the thermally assisted mechanical rupture of Zn-thiolate bonds. The Bell-Evans model (15,16) shows that the width of the unfolding force distribution is mainly determined by the distance between the bound state and the mechanical rupture transition state (Δx_u), whereas the average rupture force is determined by the energy barrier for bond rupture as well as the Δx_u.

In the experiments presented here, the mechanical rupture of the ZnS_4 center is not at equilibrium, as the stretching and relaxation traces show pronounced hysteresis (Fig. 4 *A*). Therefore, the mechanical rupture force is dependent on the pulling velocity. The higher the pulling velocity, the higher is the mechanical rupture force (Fig. 4 *B*), a behavior that is similar to the mechanical unfolding of proteins as well as the rupture of a variety of chemical bonds (16,18,19,42).

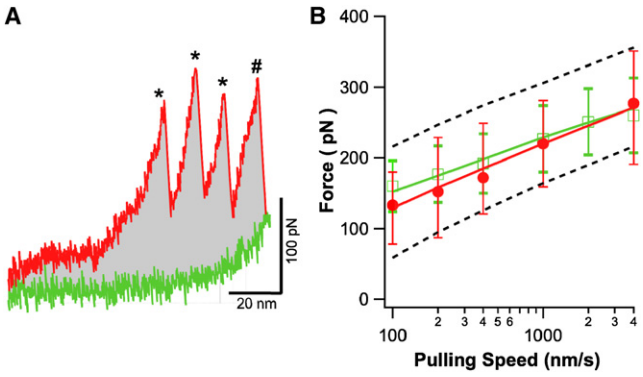

FIGURE 4 Mechanical rupture of Zn-thiolate bonds in Zn-*pf*RD is a nonequilibrium process. (*A*) A typical pair of stretching (*dark colored*) and relaxation (*light colored*) curves of polyprotein (Zn-*pf*RD-GB1)$_n$. Unfolding events of Zn-*pf*RD are indicated by *, and the unfolding event of GB1 is indicated by #. A clear hysteresis (*shaded area*) between the stretching and relaxation curves is evident. (*B*) Pulling-speed dependence of the mechanical rupture force of Zn-thiolate bonds in Zn-*pf*RD (in *dark color*). For comparison, the pulling-speed dependence for the mechanical unfolding force of GB1 is also shown (in *light color*). Solid lines are Monte Carlo simulation results obtained with $\alpha_0 = 0.1\ s^{-1}$ and $\Delta x_u = 0.14$ nm for the mechanical rupture of Zn-thiolate bonds, and $\alpha_0 = 0.03\ s^{-1}$ and $\Delta x_u = 0.17$ nm for mechanical unfolding of GB1 domains, respectively. To illustrate the relative error in the estimated α_0 and Δx_u, Monte Carlo simulation results obtained with $\Delta x_u = 0.14$ nm, and $\alpha_0 = 0.01 s^{-1}$ and $1\ s^{-1}$ are also plotted (*dotted lines*).

Because there is no analytical solution for the unfolding force distribution or its pulling speed dependence measured for polyproteins from force-extension experiments, we used a well-established Monte Carlo simulation protocol (35) to replicate the mechanical rupture of Zn-thiolate bonds and the unfolding of Zn-*pf*RD. We found that the rupture force histogram and the pulling speed dependence of the mechanical rupture force can be well described by a spontaneous dissociation rate constant α_0 of $0.10\ s^{-1}$ at zero force and a Δx_u of 0.14 nm. To illustrate the relative error within obtained values of α_0 and Δx_u, we also show Monte Carlo simulation data generated with different α_0 and Δx_u (Fig. 4 *B*).

Of note, the relatively large dissociate rate constant ($0.10\ s^{-1}$) for Zn-thiolate bonds in RD is consistent with the reported kinetic lability of the ZnS_4 site ($0.15\ s^{-1}$) (8,43,44). In fact, only a few Zn tetra-alkylthiolate complexes, which serve as a model for the structural site of the ZnS_4 site in Zn metalloproteins, have been chemically synthesized and characterized. All of these analogs are coordinated by bidentate ligands or within a peptide structure (43,45,46). The big contrast between the small number of Zn tetra-alkylthiolate complexes presently synthesized versus commonly observed ZnS_4 centers in proteins suggests that the protein environment may play a more important role in stabilizing the ZnS_4 center than does $Zn(SCH_2R)_4$, possibly by reducing the entropy that occurs when four ligands are brought together to form the ZnS_4 center.

Mechanically ruptured Zn-thiolate bonds can readily reform

In contrast to synthetic analogs that mimic metal centers in proteins, metalloproteins possess the unique ability to spontaneously fold and form their corresponding metal center. In principle, the ZnS_4 center in Zn-*pf*RD should be able to reconstitute spontaneously after unfolding. However, the nature of the broken Zn-thiolate bonds remains unknown, with no free Zn^{2+} in solution after unfolding. If all four Zn-thiolate bonds break during the mechanical rupture process, Zn^{2+} could diffuse away and prevent the reconstitution of the ZnS_4 center. If Zn^{2+} remains attached to one or more cysteine residues after mechanical rupture is completed, it is possible that the ZnS_4 center can be reconstituted.

To examine these possibilities, we carried out single-molecule refolding experiments by repeatedly stretching and relaxing the same (Zn-*pf*RD-GB1)$_n$ polyprotein for multiple cycles, as shown in Fig. 5. In curve *a*, the presence of the unfolding event with ΔLc of 13 nm indicates that one Zn-*pf*RD domain was unfolded and its ZnS_4 center ruptured. After it was relaxed to zero extension for 1 s, the polyprotein chain was stretched again. In the resultant force-extension curves (curves *b* and *c*), the unfolding event with a ΔLc of

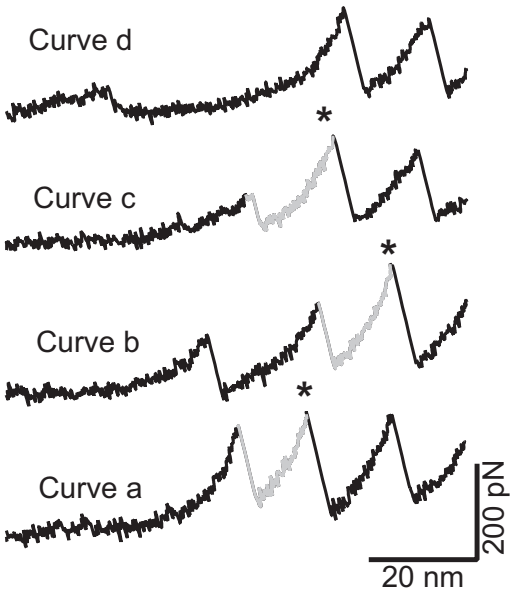

FIGURE 5 Four consecutive stretching and relaxation curves of $(Zn\text{-}pf\text{RD-GB1})_n$. The unfolding event of Zn-*pf*RD is colored in gray. In curve *a*, one Zn-*pf*RD unfolding event was observed. After relaxation to zero force, the polyprotein was again stretched. In curves *b* and *c*, the Zn-*pf*RD unfolding event was again observed, suggesting that the Zn-thiolate bonds reformed in the Zn-*pf*RD domain. In contrast, in curve *d*, the Zn-thiolate bonds did not reform and the ZnS_4 center failed to reconstitute, as evidenced by the lack of the unfolding event of ΔLc of ~13 nm.

13 nm is observed, suggesting that the unfolded Zn-*pf*RD domain managed to refold and the ZnS_4 center reconstituted. This result suggests that the broken Zn-thiolate bonds can indeed reform to reconstitute the ZnS_4 center. Additionally, it is likely that after mechanical rupture, at least one Zn-thiolate bond remains intact. This result agrees with previous research indicating that binding of Fe(II) to two cysteines at one CXXC loop is the first step in the complete reconstitution of the FeS_4 center in RD (47).

In curve *d* of Fig. 5, we can see that the Zn-*pf*RD domain failed to show an unfolding peak of $\Delta Lc = 13$ nm, suggesting that the ZnS_4 center failed to reconstitute for this Zn-*pf*RD domain. We are currently investigating the reconstitution kinetics of ZnS_4 using a well-established double-pulse, single-molecule AFM protocol (36,40).

DISCUSSION

Comparing the mechanical stabilities of Zn-S and Zn-N bonds

In this study, we used single-molecule AFM techniques to directly measure the rupture force of the Zn-S (Zn-thiolate) bond (~170 pN). To our best knowledge, this is the first direct measurement of the mechanical strength of Zn-thiolate bond. Most measurements of coordination bonds involving Zn have focused on Zn-N bonds using an NTA-his-tag system (21), largely due to the ease of preparing such systems for single-molecule AFM experiments. In contrast to these prior measurements, our study reveals unambiguous, single-molecule stretching signatures, and hence provides a general methodology to investigate the mechanical strength of metal-thiolate bonds in a protein environment.

It is noted that the mechanical rupture force of Zn-thiolate bonds is significantly higher than the reported rupture force for Zn-N (Zn-histidine) bonds (~30 pN) (13,21). This difference may be explained by the chemical nature of Zn-S and Zn-N bonds. It is well known that Zn(II)-ligand bonds are dominated by electrostatic interactions and have a small degree of covalency (43). Thus, stronger bonding is expected for Zn(II) and negatively charged anionic thiolate ligands than for Zn(II) and the neutral histidine ligand. This difference gives rise to the higher mechanical stability found for Zn-thiolate bonds.

The difference in mechanical stability between Zn-N and Zn-S bonds may also have implications for the structural role of the CXXC motif in metalloproteins. It is known that the ZnS_4 site, which is coordinated by four thiolate ligands, mainly plays a structural role in proteins (3,48). Additionally, the CXXC motif, which contains a pair of cysteines, is widely present alongside histidine ligands within Zn-containing proteins. For example, one CXXC motif and one HXXH motif form the best-known metal-coordinating pattern in the classic Zn finger protein as the C_2H_2 site (1,5,49). Considering the low mechanical stability of Zn-N bonds (Zn-histidine), it is likely that the Zn-thiolate bonds in the CXXC motif help connect specific parts of the protein together, providing rigidity to the center so that it can function as an important structural motif.

Comparison of Zn-thiolate bonds and Fe-thiolate bonds

Our study lends to an interesting comparison between Zn-thiolate bonds and Fe-thiolate bonds in RD. In Zn^{2+}, the d-orbital is completely filled. Thus, the Zn-thiolate bond is largely dominated by electrostatic interactions. In contrast, Fe-thiolate bonds are highly covalent due to the large degree of electron sharing between the tetrathiolate ligand and Fe^{3+} (43,50). Despite the different natures of Zn-thiolate and Fe-thiolate bonds, their mechanical stabilities are similar, suggesting that covalency is not the determining factor in the mechanical stability of these bonds.

It is also of note that the distance to the rupture transition state Δx_u of Zn-thiolate bonds (0.14 nm) is longer than that of Fe bonds (0.11 nm). The longer Δx_u suggests that Zn-thiolate bonds can tolerate longer bond separation upon dissociation, and the mechanical rupture force is less sensitive to the pulling velocity. However, it remains to be established whether this difference in Δx_u can be explained by the variation in bond nature between these two metal-thiolate

bonds. In the same vein, it will be important to delineate the molecular/atomic determinants for mechanical properties (including mechanical rupture force, dissociation rate constant at zero force, and distance to the rupture transition state Δx_u) of metal-thiolate bonds in metalloproteins using different metal-substituted RDs (25). The methodology reported here proves that such endeavors are possible.

CONCLUSION

In this work, we used single-molecule AFM to directly probe the mechanical stability of the Zn-thiolate bond in Zn-*pf*RD. We found that Zn-thiolate bonds rupture at ~170 pN, which is considerably larger than the rupture force of the coordination bond Zn-N (Zn-histidine). We also observed that the ZnS_4 center can be reconstituted spontaneously after the mechanical rupture of Zn-thiolate bonds in Zn-*pf*RD. To our knowledge, this study provides new information about the Zn-thiolate bond in proteins and opens a new avenue for studying metal-ligand bonds in proteins using single-molecule AFM.

We thank Prof. Pierre Kennepohl and Prof. Grant Mauk for stimulating discussions, and Ashlee Jollymore for a critical reading of the manuscript.

This work was supported by the Natural Sciences and Engineering Research Council of Canada, the Canada Foundation for Innovation, and the Canada Research Chairs Program.

REFERENCES

1. Miller, J., A. D. McLachlan, and A. Klug. 1985. Repetitive zinc-binding domains in the protein transcription factor IIIA from *Xenopus* oocytes. *EMBO J.* 4:1609–1614.
2. Berg, J. M., and Y. G. Shi. 1996. The galvanization of biology: a growing appreciation for the roles of zinc. *Science.* 271:1081–1085.
3. Andreini, C., L. Banci, …, A. Rosato. 2006. Counting the zinc-proteins encoded in the human genome. *J. Proteome Res.* 5:196–201.
4. Maret, W., and Y. Li. 2009. Coordination dynamics of zinc in proteins. *Chem. Rev.* 109:4682–4707.
5. Auld, D. S. 2001. Zinc coordination sphere in biochemical zinc sites. *Biometals.* 14:271–313.
6. Cox, E. H., and G. L. McLendon. 2000. Zinc-dependent protein folding. *Curr. Opin. Chem. Biol.* 4:162–165.
7. Petros, A. K., A. R. Reddi, …, B. R. Gibney. 2006. Femtomolar Zn(II) affinity in a peptide-based ligand designed to model thiolate-rich metalloprotein active sites. *Inorg. Chem.* 45:9941–9958.
8. Reddi, A. R., and B. R. Gibney. 2007. Role of protons in the thermodynamic contribution of a Zn(II)-Cys4 site toward metalloprotein stability. *Biochemistry.* 46:3745–3758.
9. Sénèque, O., and J. M. Latour. 2010. Coordination properties of zinc finger peptides revisited: ligand competition studies reveal higher affinities for zinc and cobalt. *J. Am. Chem. Soc.* 132:17760–17774.
10. Buchsbaum, J. C., and J. M. Berg. 2000. Kinetics of metal binding by a zinc finger peptide. *Inorg. Chim. Acta.* 297:217–219.
11. Berg, J. M., and H. A. Godwin. 1997. Lessons from zinc-binding peptides. *Annu. Rev. Biophys. Biomol. Struct.* 26:357–371.
12. Janshoff, A., M. Neitzert, …, H. Fuchs. 2000. Force spectroscopy of molecular systems-single molecule spectroscopy of polymers and biomolecules. *Angew. Chem. Int. Ed. Engl.* 39:3212–3237.
13. Beyer, M. K., and H. Clausen-Schaumann. 2005. Mechanochemistry: the mechanical activation of covalent bonds. *Chem. Rev.* 105:2921–2948.
14. Kienberger, F., A. Ebner, …, P. Hinterdorfer. 2006. Molecular recognition imaging and force spectroscopy of single biomolecules. *Acc. Chem. Res.* 39:29–36.
15. Bell, G. I. 1978. Models for the specific adhesion of cells to cells. *Science.* 200:618–627.
16. Evans, E., and K. Ritchie. 1997. Dynamic strength of molecular adhesion bonds. *Biophys. J.* 72:1541–1555.
17. Grandbois, M., M. Beyer, …, H. E. Gaub. 1999. How strong is a covalent bond? *Science.* 283:1727–1730.
18. Florin, E. L., V. T. Moy, and H. E. Gaub. 1994. Adhesion forces between individual ligand-receptor pairs. *Science.* 264:415–417.
19. Ainavarapu, S. R., J. Brujic, …, J. M. Fernandez. 2007. Contour length and refolding rate of a small protein controlled by engineered disulfide bonds. *Biophys. J.* 92:225–233.
20. Caruso, M. M., D. A. Davis, …, J. S. Moore. 2009. Mechanically-induced chemical changes in polymeric materials. *Chem. Rev.* 109: 5755–5798.
21. Schmitt, L., M. Ludwig, …, R. Tampé. 2000. A metal-chelating microscopy tip as a new toolbox for single-molecule experiments by atomic force microscopy. *Biophys. J.* 78:3275–3285.
22. Conti, M., G. Falini, and B. Samorì. 2000. How strong is the coordination bond between a histidine tag and Ni-nitrilotriacetate? An experiment of mechanochemistry on single molecules. *Angew. Chem. Int. Ed. Engl.* 39:215–218.
23. Kienberger, F., G. Kada, …, P. Hinterdorfer. 2000. Recognition force spectroscopy studies of the NTA-His6 bond. *Single Mol.* 1:59–65.
24. Zheng, P., and H. Li. 2011. Highly covalent ferric-thiolate bonds exhibit surprisingly low mechanical stability. *J. Am. Chem. Soc.* 133: 6791–6798.
25. Maher, M., M. Cross, …, A. G. Wedd. 2004. Metal-substituted derivatives of the rubredoxin from *Clostridium pasteurianum*. *Acta Crystallogr.* 60:298–303.
26. Blake, P. R., J. B. Park, …, M. W. Adams. 1991. Determinants of protein hyperthermostability: purification and amino acid sequence of rubredoxin from the hyperthermophilic archaebacterium *Pyrococcus furiosus* and secondary structure of the zinc adduct by NMR. *Biochemistry.* 30:10885–10895.
27. Eidsness, M. K., S. E. O'Dell, …, R. A. Scott. 1992. Expression of a synthetic gene coding for the amino acid sequence of *Clostridium pasteurianum* rubredoxin. *Protein Eng.* 5:367–371.
28. Blake, P. R., J. B. Park, …, M. F. Summers. 1992. Solution-state structure by NMR of zinc-substituted rubredoxin from the marine hyperthermophilic archaebacterium *Pyrococcus furiosus*. *Protein Sci.* 1:1508–1521.
29. George, G. N., I. J. Pickering, …, M. W. W. Adams. 1996. X-ray absorption spectroscopy of *Pyrococcus furiosus* rubredoxin. *J. Biol. Inorg. Chem.* 1:226–230.
30. Holm, R. H., P. Kennepohl, and E. I. Solomon. 1996. Structural and functional aspects of metal sites in biology. *Chem. Rev.* 96:2239–2314.
31. Myers, L. C., G. L. Verdine, and G. Wagner. 1993. Solution structure of the DNA methyl phosphotriester repair domain of *Escherichia coli* Ada. *Biochemistry.* 32:14089–14094.
32. Maret, W. 2004. Zinc and sulfur: a critical biological partnership. *Biochemistry.* 43:3301–3309.
33. Wastl, J., H. Sticht, …, S. Hoffmann. 2000. Identification and characterization of a eukaryotically encoded rubredoxin in a cryptomonad alga. *FEBS Lett.* 471:191–196.
34. Zheng, P., Y. Cao, and H. Li. 2011. Facile method of constructing polyproteins for single-molecule force spectroscopy studies. *Langmuir.* 27:5713–5718.

35. Rief, M., J. M. Fernandez, and H. E. Gaub. 1998. Elastically coupled two-level systems as a model for biopolymer extensibility. *Phys. Rev. Lett.* 81:4764.

36. Oberhauser, A. F., P. E. Marszalek, …, J. M. Fernandez. 1998. The molecular elasticity of the extracellular matrix protein tenascin. *Nature.* 393:181–185.

37. Carrion-Vazquez, M., A. F. Oberhauser, …, J. M. Fernandez. 1999. Mechanical and chemical unfolding of a single protein: a comparison. *Proc. Natl. Acad. Sci. USA.* 96:3694–3699.

38. Carrion-Vazquez, M., A. F. Oberhauser, …, J. M. Fernandez. 2000. Mechanical design of proteins studied by single-molecule force spectroscopy and protein engineering. *Prog. Biophys. Mol. Biol.* 74:63–91.

39. Cao, Y., C. Lam, …, H. Li. 2006. Nonmechanical protein can have significant mechanical stability. *Angew. Chem. Int. Ed. Engl.* 45: 642–645.

40. Cao, Y., and H. Li. 2007. Polyprotein of GB1 is an ideal artificial elastomeric protein. *Nat. Mater.* 6:109–114.

41. Marko, J. F., and E. D. Siggia. 1995. Stretching DNA. *Macromolecules.* 28:8759–8770.

42. Rief, M., M. Gautel, …, H. E. Gaub. 1997. Reversible unfolding of individual titin immunoglobulin domains by AFM. *Science.* 276:1109–1112.

43. Picot, D., G. Ohanessian, and G. Frison. 2010. Thermodynamic stability versus kinetic lability of ZnS4 core. *Chem. Asian J.* 5:1445–1454.

44. Wilker, J. J., and S. J. Lippard. 1997. Alkyl transfer to metal thiolates: kinetics, active species identification, and relevance to the DNA methyl phosphotriester repair center of *Escherichia coli* Ada. *Inorg. Chem.* 36:969–978.

45. Parkin, G. 2004. Synthetic analogues relevant to the structure and function of zinc enzymes. *Chem. Rev.* 104:699–767.

46. Rao, C. P., J. R. Dorfman, and R. H. Holm. 1986. Synthesis and structural systematics of ethane-1,2-dithiolato complexes. *Inorg. Chem.* 25:428–439.

47. Morleo, A., F. Bonomi, …, D. M. Kurtz, Jr. 2010. Iron-nucleated folding of a metalloprotein in high urea: resolution of metal binding and protein folding events. *Biochemistry.* 49:6627–6634.

48. Karlin, S., and Z. Y. Zhu. 1997. Classification of mononuclear zinc metal sites in protein structures. *Proc. Natl. Acad. Sci. USA.* 94:14231–14236.

49. Lu, D., M. A. Searles, and A. Klug. 2003. Crystal structure of a zinc-finger-RNA complex reveals two modes of molecular recognition. *Nature.* 426:96–100.

50. Solomon, E. I., S. I. Gorelsky, and A. Dey. 2006. Metal-thiolate bonds in bioinorganic chemistry. *J. Comput. Chem.* 27:1415–1428.